Available online at www.sciencedirect.com

SciVerse ScienceDirect

Ceramics International 39 (2013) 483–488

CERAMICS INTERNATIONAL

www.elsevier.com/locate/ceramint

Influence of mechanical activation on sphene based ceramic material synthesis

Jelena Pantić[a,*], Aleksandar Kremenović[b], Anja Došen[a], Marija Prekajski[a], Nadežda Stanković[a], Zvezdana Baščarević[c], Branko Matović[a]

[a]Department of Material Science, INS Vinča, University of Belgrade, P.O. Box 522, Belgrade, Serbia
[b]Faculty of Mining and Geology, University of Belgrade, Djušina 7, Belgrade, Serbia
[c]Center for Multidisciplinary Studies, University of Belgrade, Kneza Višeslava 1, Belgrade, Serbia

Received 19 February 2012; received in revised form 15 June 2012; accepted 16 June 2012
Available online 28 June 2012

Abstract

Sphene ($CaTiSiO_5$), a calcium titanosilicate ceramic has been prepared from a powder mixture of $CaCO_3$, TiO_2 and SiO_2 using vibro-milling for homogenization and activation of precursors. The mechanochemical process initially yielded amorphous powders, which on further calcination, crystallized to yield sphene ceramic. The evolution of the phase composition with thermal treatment was investigated by X-ray powder diffraction (XRPD). Powder morphology and particle size distribution were analyzed by scanning electron microscopy (SEM) and laser diffraction, respectively. Rietveld refinement was employed to get the structural information of the synthesized powder. Densification and microstructure evolution was determined by means of density and scanning electron microscopy (SEM). The most favorable conditions for mechanical activation and synthesis of sphene based ceramic material are reported.

Keywords: Sphene; Mechanochemistry; Rietveld refinement; SEM/EDS

1. Introduction

Sphene or titanite is a nesosilicate mineral with monoclinic symmetry. It can crystallize both as primary (space group $A2/a$) and lower-T phase (space group $P2_1/a$). The ideal chemical formula of sphene can be written as $CaTiSiO_5$ or $CaTiO(SiO_4)$ [1]. However, within the structure, significant substitutions in both cation and anion sites may occur. Calcium, in coordination 7, can be replaced with Mn [2], then Sr, Ba, rare earth elements and Th when high valence is compensated by joining Fe^{3+} and Al by Ti [3]. Titanium, in coordination 6, can be replaced with Al^{3+} [4], Fe^{3+} [5], Ta [6] and Nb [7,8] compensating the charge difference by incorporating Na instead of Ca. Dual substitution of Fe and Al with Ti and OH, Cl, F, with O, are only possible in natural sphene [9,10]. Ribbe [11] noted that all Ti atoms are moved out from their geometric center in octahedrons in the same direction along the axis a, which is reflected in structure geometry i.e. longer and shorter Ti–O bonds.

Because of the distorted TiO_6 octahedra and consequent low point symmetry, titanite is desirable to develop an intense coloration [12]. Ones that contain Cr^{3+} are used as pink pigment for painting ceramics in pink and purple [13]. Furthermore, titanite also has a good thermal stability and it is an excellent candidate for a host lattice of ceramic materials [14]. It can also be used for nuclear waste disposal [15–17] or luminescent materials [18], since it is possible to incorporate a variety of elements into its crystal lattice. In high concentrations sphene is a potential source of titanium [19].

It is very difficult to obtain pure synthetic monophase titanite. Many different methods such as: sol–gel [20], coprecipitation [20], combustion [21], spray pyrolysis [22], freeze-drying [23] and hydrothermal methods have been used. In most cases pure sphene was not obtained. There are always some traces of crystobalite (SiO_2), perovskite ($CaTiO_3$), wollastonite ($CaSiO_3$) and other phases, besides sphene.

*Corresponding author. Tel.: +381 11 3408 782.
E-mail address: jelena.pantic@vinca.rs (J. Pantić).

0272-8842/$36.00
http://dx.doi.org/10.1016/j.ceramint.2012.06.052

The aim of this work is to explore the influence of mechanochemical activation of precursors prior to synthesis of sphene. Publications cover mostly grinding of natural sphene concentrates [24,25]. Mechanochemistry represents an alternative route in synthesis of sphene. So far, many materials are synthesized by this method in the form of nanoparticles and nanocrystalline powders [26]. In this study, vibratory mills are used. They are classed with grinding devices operating via impact and attrition. In such mills the impact is produced by the grinding body sliding over the material being ground or rotating around some axis. Mechanochemical routes are attractive because of their simplicity, flexibility, and ability to prepare materials by solid state reactions at room temperature [27]. Finally, it is simpler and easier to implement this method in industrial level.

2. Experimental methods

2.1. Powder preparation

Reactants used in the synthesis are commercially obtained powders: TiO_2 (Lab. Art. 808E. Merck), SiO_2 (ASP-K-amorphous, Prahovo) and $CaCO_3$ (pro analysi, 11490, Kemika, Zagreb). All precursors have been dried at 105 °C for 24 h and stored in an exsicator to avoid atmospheric moisture before weighing. Four samples were prepared from stoichiometric amounts of these powders in order to obtain 5 g of sphene (2.5529 g TiO_2, 2.0344 g SiO_2, 1.5324 g $CaCO_3$). The powder mixtures were homogenized in the vibratory mill (Fritsch Pulverisette Analysette Laborette, type 09 003, no. 155, 380 V). The Vibratory Pulverizer uses ring ($\varnothing = 5.3$ cm, $h = 4.3$ cm) and a disk ($\varnothing = 10.3$ cm, $h = 4.3$ cm) inside a hard-metal tungsten carbide grinding bowl ($\varnothing = 13$ cm, $h = 6.3$ cm). Volume of the container is 100 ml with $m = 3200$ g. The device can operate at two speeds of vibration: 750 min^{-1} and 1000 min^{-1}. Samples were ground up to 2 h in air atmosphere (15 min, 30 min, 1 h and 2 h) with speed of 750 min^{-1}.

Five pellets were made from each sample for different grinding time ($\varnothing = 8$ mm, $h = 5$ mm). They were obtained by hydraulic pre-pressing under the pressure of 100 MPa. Sintering of compacted powders was carried out at different temperatures (from 900 to 1300 °C) in air at a heating rate of 10 °C/min and a soaking period of 2 h in alumina crucibles.

2.2. Characterization

Before any calcinations, the average particle size and particle size distribution were determined by particle size analyzer (PSA) using Mastersizer 2000 (Malvern Instruments Ltd., UK). Particle size analyzer, based on laser diffraction, covers the particle size range of 0.02–2000 μm. For the PSA measurements, the powders were dispersed in distilled water, in an ultrasonic bath (low-intensity ultrasound, at a frequency of 40 kHz and power of 50 W), for 5 min.

The sintered pellets were polished and thermally etched at temperature of 1150 °C for 30 min. Microstructure and chemical composition were investigated with Au/Pd coating using a scanning electron microscope (SEM) Vega TS 5130 MM, Tescan, coupled by EDS (INCA PentaFET-x3, Oxford Instruments).

Determination of the melting point of sintered sphene was followed by hot-stage microscopy (HSM) using Carl Zeiss-Jena termomicroscop with PtPt-Rh termocouple in range of 20–1350 °C.

All of the powders were characterized at room temperature by X-ray powder diffraction (XRPD) using Siemens D-500 diffractometer. Cu $K_{\alpha 1,2}$ radiation was used in conjunction with a Cu K_β nickel filter. The range of 10–90°2θ was used for all powders with a scanning step size of 0.02°.

Data for structural refinement were taken in the 2θ range 10–90°2θ, with the step of 0.02° and scanning time of 12 s per step. The refinement was performed with the FullProf computer program which adopts the Rietveld calculation method. The TCH pseudo-Voigt profile function was used.

3. Results and discussion

It is well known that grinding has a significant place in the processing of ceramic materials. It leads to physical and chemical changes in materials and in that case, grinding is referred to as mechanochemical treatment [28]. Mechanically induced violation of the mineral grain structure is accompanied by reduction of the size of the mineral particles and the associated increase in the specific surface area, accumulation of free energy on the particles and, thereby, by enhancement of the chemical activity of the surface layer [29].

In the volumetric size distribution (Fig. 1), sample with grinding time of 1 h shows the best uniformity, next is sample with grinding time of 30 min, then with 2 h grinding and in the end the one with 15 min of grinding.

Theoretical density was calculated for each sample after sintering. It was shown that the highest density have samples with grinding time of 30 min on 1200 °C and 1250 °C (Table 1). With the sintering temperature of 1200 °C the density is 3.33 g/cm^3 which represents ~95% of the theoretical value.

Sintering above 1300 °C leads to melting of the material (Fig. 2). Due to results from PSA and calculated density, sample with grinding time of 30 min was chosen for further analyses.

The microstructure of the sphene with grinding time 30 min heated at 1200 °C is shown in Fig. 3(a–d). The analysis shows bimodal grain structure that is in good agreement with volumetric size distribution analysis. The average particle sizes estimated from SEM images are 3 and 5 μm. The micrographs revealed the dense nature of the compact sintered at 1200 °C with the irregular shaped and elongated grains. Vibratory mills are very efficient as

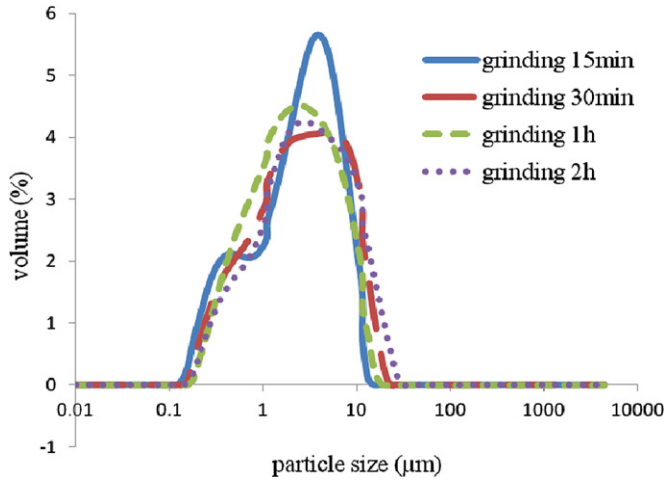

Fig. 1. Particle size distribution curves for samples with different grinding times.

Table 1
Densities of sphene vs. annealing time.

Grinding time				
T (°C)	**15 min**	**30 min**	**1 h**	**2 h**
900	2.04 g/cm^3	1.69 g/cm^3	0.98 g/cm^3	0.77 g/cm^3
1000	2.12 g/cm^3	1.76 g/cm^3	1.04 g/cm^3	0.76 g/cm^3
1100	1.61 g/cm^3	2.16 g/cm^3	1.18 g/cm^3	1.13 g/cm^3
1200	2.93 g/cm^3	3.33 g/cm^3	2.67 g/cm^3	2.31 g/cm^3
1250	2.59 g/cm^3	3.34 g/cm^3	2.74 g/cm^3	2.35 g/cm^3

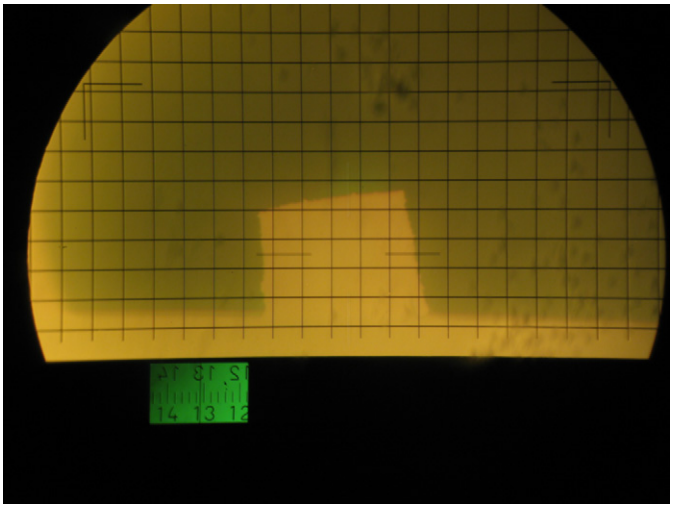

Fig. 2. Selected HSM image of the sample that was mechanochemically activated 30 min above 1300 °C during firing.

regards to the achievement of the desired particle size of the titanite particles (< 10 μm) [26].

The order of abundance Ca, Ti, Si and O suggests sphene. Ca, Si and Ti elements were evident in the sphene, as indicated by the EDS analysis.

The XRPD of the sample that was mechanochemically activated 30 min (Fig. 4) depicts the formation of sphene ($CaTiSiO_5$) as a principle crystalline phase at 900 °C. The main reflections in these patterns are observed at 2θ of 17, 27, 29, and 34°, which is typical for the titanite structure. Perovskite ($CaTiO_3$), a secondary phase, was detected. On further increasing the temperature up to 1000, 1100 and 1200 °C, the intensity of sphene reflections increased, due to better crystallization, whereas the perovskite reflections decreased. However, the secondary phase is present at all temperatures indicating its minor amounts. The third phase, coesite (SiO_2), was noticed during XRPD measurements with high sensitive condition and in the Rietveld refinement. The perovskite phase is thermodynamically unstable at high temperatures and probably its decomposition provokes titanite crystal growth [22]. No amorphous phase was detected during XRPD analysis, which indicates that some amount of perovskite reacted with SiO_2 and recrystallized to form sphene. That confirms the decreasing of perovskite reflections intensities.

Sample that was mechanochemically activated 30 min and heated at 1200 °C was selected in order to refine their structural and microstructural parameters using the Fullprof program [30,31], which allows refining the lattice parameters, atomic coordinates, and microstructural parameters simultaneously. Graphic result of Rietveld structural refinement as the best fit between calculated and observed X-ray diffraction pattern is shown in Fig. 5. Refined crystallographic parameters of all phases with corresponding agreement factors and microstructure parameters are given in Table 2. All the structure models i.e. cif files for refinement are taken from the American Mineralogist Crystal Data Structure Base (AMCDSB) [32]. Sphene crystallizes as lower-T phase (space group $P2_1/a$), which is very common for synthetic sphene [8]. Besides sphene, microstructural parameters are also refined for perovskite and coesite. Perovskite crystallizes in *Pbnm* space group, while coesite crystallizes in $C\ 2/c$ space group. To take instrumental broadening into account, the XRPD pattern of a standard specimen CeO_2 was fitted by the convolution of the experimental TCH pseudo-Voigt function [33]. Values of average apparent crystallite size obtained by the refinement of the TCH-pV parameters for all phases are also given in Table 2. The average particle size estimated from XRPD data for sphene is smaller than the average particle size computed by SEM, suggesting that the particles are composed of packed crystallites.

Quantitative analysis was done by Reitveld refinement due to XRPD analysis. Percentage of each phase calculated from the Rietveld refinement is 93.3% for sphene, 2.9% for perovskite and 3.8% for coesite. These results are for sphene after sintering at 1200 °C when titanite reaches 93.3% wt as a major crystalline phase.

Table 3 shows fractional atomic parameters of refined sphene, while Table 4 depicts interatomic distances. The distances Ti–O, Si–O, Ca–O in space group $P2_1/a$ show good agreement with literature data [4,9]. The distorted

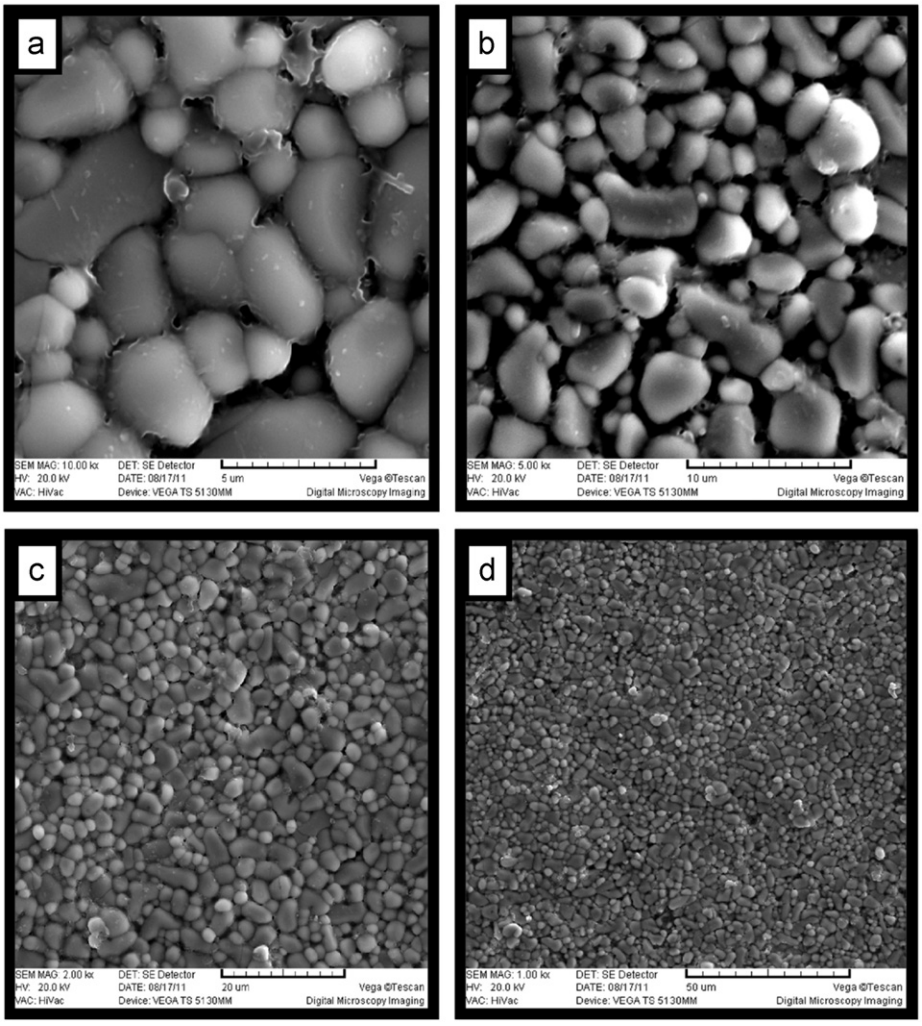

Fig. 3. SEM micrographs at different magnification of sphene (a, b, c, d) with grinding time 30 min heated at 1200 °C.

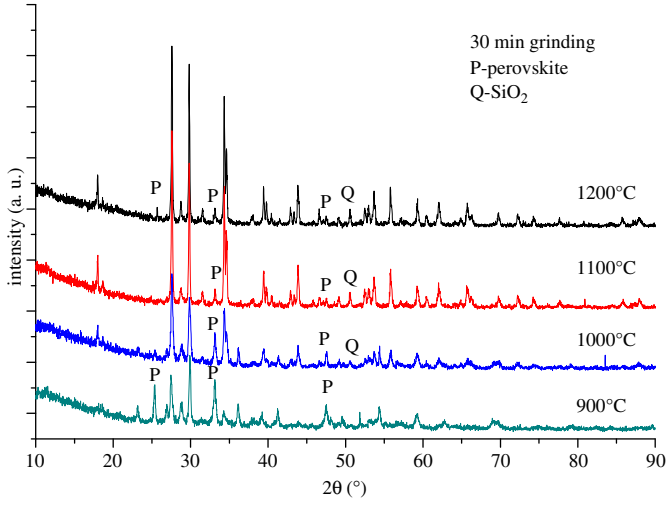

Fig. 4. X-ray diffraction patterns of sphene (30 min grinding) after heating at different temperatures. Symbols: P—$CaTiO_3$, Q—SiO_2. The sphene peaks have not been labeled.

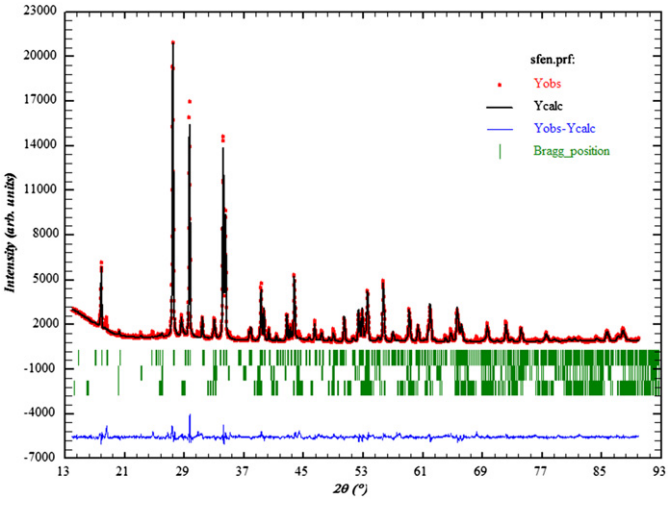

Fig. 5. Rietveld refinement plot of the X-ray powder diffraction data of the sphene heated at 1200 °C. In the figure the continuous line represents the calculated pattern, while circles show the observed pattern. The residual curve is plotted below. Vertical bars represent reflection positions: first row sphene, second row perovskite and third row coesite.

Table 2
Refined structural and microstructural parameters for each phase and corresponding agreement factors. Crystallite size and strain values for perovskite and coesite assumed to be equal.

Space group symbol	*$P2_1/a$*	*Pbnm*	*C 2/c*
Lattice parameters (Å)	***sphene***	***perovskite***	***coesite***
a	7.05442 (6)	5.3901 (8)	7.1397 (13)
b	8.71998 (8)	5.4468 (8)	12.450 (3)
c	6.56133 (6)	7.6715 (8)	7.2325 (8)
α, γ	90	90	90
β	113.756 (2)	90	120.467 (11)
ρ (g/cm^3)	3.532	4.026	2.903
Vol (Å^3)	368.662 (2)	224.345 (7)	549.894 (2)
Crystallite size (nm)	514 (5)	86 (1)	86 (1)
Strain (10^4)	15.582	17.645	17.645
Agreement factors			
R_p	14.5		
wR_p	13.9		
R_{exp}	6.47		
χ^2	4.61		

Table 3
Fractional atomic parameters estimated standard deviation (in parentheses) for sphene.

	x	*y*	*z*
Ti	0.5147 (11)	0.7450 (9)	0.2448 (10)
Ca	0.2599 (10)	0.9158 (3)	0.7550 (15)
Si	0.7323 (15)	0.9344 (5)	0.7448 (17)
O (1)	0.753 (4)	0.8203 (8)	0.253 (4)
O (2)	0.9090 (12)	0.8191 (10)	0.9457 (12)
O (3)	0.389 (2)	0.9502 (16)	0.145 (2)
O (4)	0.9080 (15)	0.3115 (11)	0.4197 (15)
O (5)	0.3774 (20)	0.4808 (14)	0.647 (3)

Table 4
Interatomic distances nm (experimental data) with estimated standard deviation (in parentheses) for sphene.

Bond	**Experimental values (nm)**
$Ti–O_1$	0.179 (3)
$Ti–O_1$	0.195 (3)
$Ti–O_2$	0.1979 (2)
$Ti–O_3$	0.2133 (15)
$Ti–O_4$	0.2124 (12)
$Ti–O_5$	0.2127 (14)
$Ca–O_1$	0.2303 (7)
$Ca–O_2$	0.2410 (4)
$Ca–O_3$	0.2364 (15)
$Ca–O_3$	0.2573 (15)
$Ca–O_4$	0.2356 (10)
$Ca–O_5$	0.248 (2)
$Ca–O_5$	0.2656 (15)
$Si–O_2$	0.1591 (8)
$Si–O_3$	0.1663 (19)
$Si–O_4$	0.1638 (2)
$Si–O_5$	0.1642 (2)

TiO_6 octahedra (longer and shorter Ti–O bonds) confirm that analyzed sphene was refined in right space group. Given the small amount of other two phases, the atomic coordinates for perovskite and coesite were fixed during the refinements.

4. Conclusions

Sphene ($CaTiSiO_5$) was successfully obtained from a mixture of TiO_2, SiO_2 and $CaCO_3$ using mehanochemical activation. The best experimental condition for preparing sphene for further calcinations and sintering process was grinding time of 30 min. The highest achieved density was obtained at 1200 °C. The microstructure revealed the presence of densely packed grains in the sintered body. This simple method proved to be suitable to get sphene based ceramic material with a high sphene grade of 93.3%. The other two phases (perovskite and coesite) are present at all temperatures indicating its minor amounts.

Acknowledgments

Financial support from the Serbian Education and Science Ministry in the Framework of projects nos. 45012 and 176016 is gratefully acknowledged.

References

[1] E.S. Dana, Manual of Mineralogy, 17th ed., John Wiley & Sons, Inc., 1959 (pp. 412–413).
[2] J. Pantić, V. Kahlenberg, V. Poharc-Logar, A. Kremenović, Natural $CaO–TiO_2–SiO_2$ based ceramics, Processing and Application of Ceramics 5 (2) (2011) 79–84.
[3] W.A. Deer, R.A. Howie, J. Zussman, Rock-forming minerals, Ortho- and Ring Silicates 1 (1962) 87–95.
[4] C.L. Hollabaugh, F.F. Foit Jr., The crystal structure of an Al-rich titanite from Grisons, Switzerland, American Mineralogist 69 (1984) 725–732.
[5] I.J. Muir, J.B. Metson, G.M. Bancroft, 57Fe Mössbauer spectra of perovskite and titanite, Canadian Mineralogist 22 (1984) 689–694.
[6] L.A. Groat, F.C. Hawthorne, R.T. Carter, T.S. Ercit, Tantalian niobian titanite from the Irgon Claim, Southeast Manitoba, Canadian Mineralogist 23 (1985) 569–571.
[7] B.J. Paul, Petr Cerny, Ron Chapman, J.R. Hinthorne, Niobian titanite from the Huron Claim pegmatite, southeastern Manitoba, Canadian Mineralogist 19 (1981) 549–552.
[8] J.B. Higgins, P.H. Ribbe, The crystal chemistry and space groups of natural and synthetic titanites, American Mineralogist 61 (1976) 878–888.
[9] .A. Speer, G.V. Gibbs, The crystal structure of synthetic titanite, $CaTiOSiO_4$, and the domain textures of natural titanites, American Mineralogist 61 (1976) 238–247.
[10] R. Obeti, D.C. Smith, G. Rossi, F. Caucia, The crystal-chemistry of high-aluminium titanites, European Journal of Mineralogy 3 (1991) 777–792.
[11] P.H. Ribbe, Titanite, in: P.H. Ribbe (Ed.), Orthosilicates, Reviews in Mineralogy, vol. 5, Mineralogical Society of America, 1982 (pp. 137–155).
[12] R. Stefani, E. Longo, P. Escribano, E. Cordoncillo, J. Garda, Developing a pink pigment for glazes, American Ceramic Society Bulletin 76 (9) (1997) 61–64.

[13] P.E. Lopez, C.G. Monzonis, A.J. Navarro, Cr–SnO_2–CaO–SiO_2-based ceramic pigments, American Ceramic Society Bulletin 63 (1984) 1492–1494.
[14] P.J. Hayward, D.C. Doern, I.M. George, Dissolution of a sphene glass–ceramic, and of its component sphene and glass phases in Ca–Na–Cl brines, Journal of the American Ceramic Society 73 (1990) (544–511).
[15] P. Hayward, E. Cechetto, Development of sphene-based glass ceramics tailored for Canadian waste disposal conditions, in: S. Topp (Ed.), Scientific Basis for Nuclear Waste Management, vol. 3, 1982 (pp. 91–98).
[16] M. Gascoune, Evidence for the stability of the potential nuclear waste host, sphene, over geological time, from uranium-lead ages and uranium series measurement, Applied Geochemistry 1 (1986) 199–210.
[17] A.E. Ringwood, S.E. Kesson, K.D. Reeve, D.M. Levins, E.J. Ramm, SYNROC, in: W. Lutze, R.C. Ewing (Eds.), Radioactive Waste Forms for the Future, 1988, pp. 233–334.
[18] M. Gaft, L. Nagli, R. Reisfeld, G. Panczer, Laser-induced time-resolved luminescence of natural titanite $CaTiOSiO_4$, Optical Materials 24 (2003) 231–241.
[19] E.R. Force, Geology of Titanium-Mineral Deposits, The Geological Society of America, Inc., Boulder, Colorado, 1991.
[20] M. Muthuraman, K.C. Patil, Synthesis, properties, sintering and microstructure of sphene, $CaTiSiO_5$: a comparative study of coprecipitation, sol–gel an combustion processes, Materials Research Bulletin 33 (4) (1998) 655–661.
[21] M. Muthuraman, N.A. Dhas, K.C. Patil, Combustion synthesis of oxide materials for nuclear waste immobilization, Bulletin of Materials Science 17 (1994) 977.
[22] T.S. Lyubenova, F. Matteucci, A.L. Costa, M. Dondi, M. Ocaña, J. Carda, Synthesis of Cr-doped $CaTiSiO_5$ ceramic pigments by spray drying, Materials Research Bulletin 44 (4) (2009) 918–924.
[23] T.S. Lyubenova, F. Matteucci, A. Costa, M. Dondi, J. Carda, Ceramic pigments with sphene structure obtained by both spray- and freeze drying techniques, Powder Technology 193 (1) (2009) 1–5.
[24] A.M. Kalinkin, E.V. Kalinkina, V.N. Makarov, Mechanical activation of natural titanite and its influence on the mineral decomposition, International Journal of Mineral Processing 69 (2003) 143–155.
[25] L.G. Gerasimova, M.V. Maslova, E.S. Shchukina, Role of mechanoactivation in preparation of mineral filler pigment from titanite, Russian Journal of Applied Chemistry 83 (12) (2010) 2081–2087.
[26] T.F. Grigorieva, A.P. Barinova, N.Z. Lyakhov, Mechanosynthesis of nanocomposites, Journal of Nanoparticle Research 5 (2003) 439–453.
[27] M. Zdujić, Mechanochemical treatment of inorganic materials, Chem. Ind. 55 (2001) 191–206 (in Serbian).
[28] E.M. Gutman, Mechanochemistry of Materials, Cambridge International Science Publishing, Cambridge, 1998 (pp. 215).
[29] E. Avvakumov, M. Senna, N. Kosova, Soft Mechanochemical Synthesis: A Basis for New Chemical Technologies, Kluwer Academic Publishers, 2001 (pp. 207).
[30] J. Rodríguez-Carvajal, FullProf Computer Program, 1998, 〈ftp://charybde.saclay.cea.fr/pub/divers/fullprof.98/windows/winfp98.zip〉.
[31] J. Rodríguez-Carvajal, Recent developments of the program FULLPROF, in Commission on Powder Diffraction (IUCr), Newsletter 26 (2001) 12–19.
[32] American Mineralogist Crystal Data Structure Base (AMCDSB), 〈http://rruff.geo.arizona.edu/AMS/amcsd.php〉.
[33] J. Rodríguez-Carvajal, Recent advances in magnetic structure determination by neutron powder diffraction, Physica B 192 (1993) 55–69.